

LiDAR Models for Archaeological Feature Detection in Maya Sites

Richard K. Ellsworth

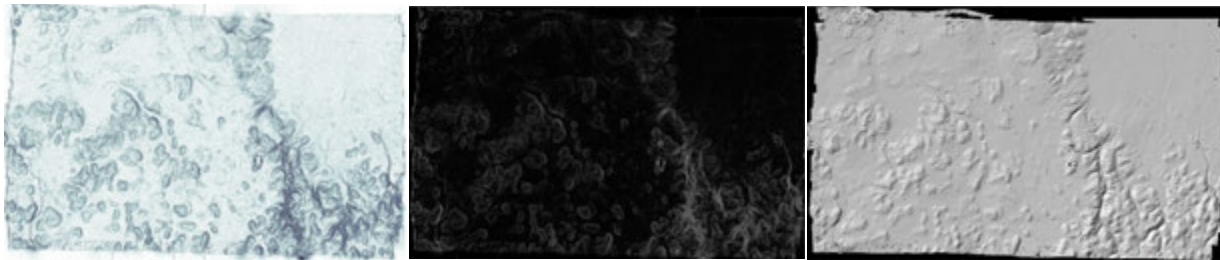
ABSTRACT: In recent years, LiDAR has become a well-established source for augmenting spatial knowledge of the archaeological landscape. In addition to being a valuable resource for terrain modeling and large feature detection, LiDAR can be used to locate and identify discrete archaeological features beneath tree canopies. Aerial laser scanning (ALS) is capable of penetrating the dense tree canopy in the Maya Forest to reveal a complex cultural landscape containing a multitude of chultuns, depressions, mounds, platforms, quarries, and terraces. ALS has been used successfully in archaeological surveys to penetrate the dense Maya Forest tree cover. Raw LiDAR data can then be rendered into several different models that are unique in their abilities to display different features. This paper explores the use of the slope model, the hillshade model, and the bonemap model (exaggerated slope values) in evaluating a series of features and their visibility in each model. Preliminary results demonstrate that certain models are more appropriate for displaying each feature type. For example, the slope map proved more successful in identifying terraces, while the bonemap is best for mounds. In this paper, features from El Pilar, a Maya site in Belize and Guatemala have been used to evaluate LiDAR efficacy.

KEYWORDS: LiDAR, GIS, archaeology, El Pilar, Maya, remote sensing, LiDAR models, bonemap, hillshade, slope map, feature visibility

Introduction

LiDAR (light detection and ranging) is based on the principle of ALS where brief, rapid laser pulses are shot at the ground from a plane or drone. Each beam then reflects back towards the aircraft source and is recorded. The amount of time taken for the laser pulse to return is converted to distance, and a point cloud image is generated of the ground surface. The raw point cloud can then be converted into a variety of useful models by filtering data values (Colluzia et al. 2011, Doneus et al., 2008, and Stular et al. 2012). This type of airborne LiDAR was used in the surveying of the pre-Columbian Maya site, El Pilar. El Pilar is an archaeological reserve for flora and fauna that is located in both Belize and Guatemala on the international boundary. The site is the largest center on the Belize River with an abundance of earthworks, most of which were erected in the Middle Pre-classic period (950 B.C.-650 B.C.) and in the Late to Terminal Classic periods (650 A.D.-1000 A.D.) (Whittaker et al. 2009). El Pilar provides a rich arena of features that yields evidence of past lifeways, land use, and forest evolution that furthers our understanding of Maya culture and landscape development. Currently, very few sites in Mesoamerica have been exposed to archaeologists, and subsequently documented and spatially analyzed. This lack of site exposure is primarily due to lack of visibility through the dense multi-

story tree canopies that dominate the Maya Forest. However, with the increasing use of LiDAR, more sites will become visible allowing archaeologists to piece together the past (Chase et al. 2010). The Maya Forest Alliance with monetary assistance from the Anfield Nickel Corporation's Mayaniquel Project (Pingel et al. 2015) collected airborne LiDAR for the 20 km² El Pilar Reserve. Since those data were collected on 19 April 2012, numerous features at El Pilar have been discovered with LiDAR derived imagery including features as small as 2 meters in diameter. This is extremely useful since many features that are characteristic of Maya sites are very small (such as chultuns and quarries) and can easily pass undetected by the human eye when covered in leaves and soil accumulation. To further improve feature visibility, Pingel and Clarke produced a bonemap rendering of the LiDAR (figure 1a). The bonemap is essentially a stretched slope map where lighting and color-coding have been altered to emphasize even the smallest of features.



(a) (b) (c)
Figure 1: (a): the bonemap model; (b) the slope model; (c) the hillshade model. All three models show the area of El Pilar analyzed in this paper.

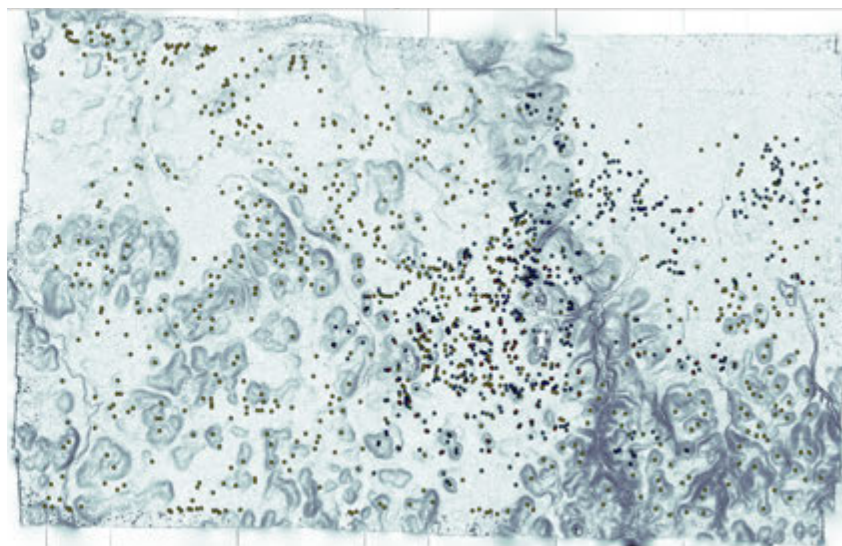


Figure 2: shows the El Pilar bonemap model with the locations of all of the shapefile points that were derived from the LiDAR. Most of these points have been groundtruthed and used in this analysis.

Using the different LiDAR models of slope (figure 1b), hillshade (figure 1c), and bonemap (figure 1a), the Mesoamerican Research Center (MARC) at the University of California Santa Barbara (UCSB) was able to generate a series of points based on the digitally observed features (figure 2). Most of those points were subsequently visited in the field, identified, and either accepted or rejected depending on their existence. With an NSF undergraduate research grant, it was possible to do a comparative analysis, assessing the visibility of each point in all three LiDAR models.

Method

To determine feature visibility, ESRI ArcMap 3.4 was used with the added layers slope, hillshade, and bonemap. The point shapefile marking all of the LiDAR identified features was also incorporated. Each point was ascribed with attributes for feature type, field acceptance or rejection, and a feature identification number. Each feature was then magnified to a close resolution of approximately 1:600 meters in each of the three layers and their visibility was assessed based on whether or not they were distinguishable as clearly different topographical features when compared to surrounding areal features. In addition to recording visibility using the labels “LiDAR identified” and “LiDAR unidentified”, the approximate size of the features was recorded as a variable. Size was determined by using the ArcMap measuring tool in the layer that displayed each feature most clearly at the 1:600-meter resolution. Mounds were measured from the base of the incline from one end to the other along a horizontal bisect. Quarries and terraces were measured in length from end to end. Depressions and chultuns were measured from the top of the decline, across the feature in a horizontal bisect to the opposite side. Finally, platforms were measured from the visible elevation change, across the area of consistent elevation to the beginning of the next elevation change. The resulting table was then joined with these added attributes to the attribute table of the LiDAR identified points. With this additional information, a select by attribute analysis was performed for each feature type (chultuns, depressions, mounds, platforms, quarries, and terraces) to determine a.) the success of the LiDAR produced points i.e. how accurate the points are in detecting features when compared to the field acceptance ratio, b.) the success of each LiDAR derived raster i.e. how effective each model is overall at displaying all 6 feature types, and c.) if any of the three rasters is more adept at identifying certain feature types than the others (see Table 1 next page).

Each query included only the LiDAR identified and field accepted features. Separate queries were conducted for each feature type, isolating the features that were visible in each individual model. The resulting number of features was then used to generate percentages of visibility when compared in a ratio to the total number of features in each category. Note that chultuns are very small, deep storage chambers used by the Maya and are difficult to spot in any LiDAR model (Weiss-Krejci and Sabbas 2002). Depressions are fairly shallow indentations that average 15 meters across, have gently sloping sides and could be chultuns (Weiss-Krejci and Sabbas 2002) (figure 3). Mounds are Maya earthworks discernable in LiDAR by a channel of lower elevation surrounding the mound (Ford and Fedick 1992) from digging and moving earth (figure 4). Platforms are areas of consistent elevation typically adjacent to mounds (figure 5). Quarries are

Table 1: illustrates the types of features and the percentages of the total number of features visible in each LiDAR model. Note that the highlighted percentages signify the model that most accurately displays each feature type and the extent to which that feature type is visible.

	Chultuns	Depressions	Mounds	Platforms	Quarries	Terraces	Total
Number of Features	35	44	449	74	115	20	737
LiDAR Identified	63%	82%	89%	75%	77%	86%	
LiDAR Identified and Field Accepted	63%	70%	80%	74%	72%	71%	75%
LiDAR Unidentified and Field Rejected	37%	30%	20%	26%	28%	29%	25%
Hillshade Visible	46%	64%	62%	42%	41%	55%	56%
Slope Visible	.06%	48%	60%	55%	43%	65%	54%
Bonemap Visible	26%	59%	72%	68%	61%	55%	67%

fairly shallow, short-in-length indentations (figure 6) that were used prehistorically and historically as a source for lithics (Ford and Fedick 1992). And finally, terraces are step-like platforms that were used for agriculture and they are LiDAR identified by adjacent, linear striations (Healy et al. 1983).



Figure 3: Large depression/aguada at El Pilar, Belize; Source: MARC at UCSB



Figure 4: House mound in a clearing at El Pilar, Belize; Source: MARC at UCSB



Figure 5: Platform in front of exposed structure at El Pilar, Belize; Source: MARC at UCSB



Figure 6: Close-up of quarry with rock exposure at El Pilar, Belize; Source: MARC at UCSB

Results

The objective to establish that certain LiDAR models are more adept at displaying different feature types than others was successful. However, the margin of success is minimal indicating that the process of using one model for any one feature type is not appropriate for producing concrete results. The primary results show that first, the LiDAR imagery overall is 75% effective at identifying features. Second, the results suggest that the bonemap model is the most effective model for identifying the highest amount of features with 67% accuracy. Third, the raw slope map is the least effective model overall. And fourth, in regard to feature types, chultuns are the most difficult features to observe with LiDAR. This is expected since they are very small, but some chultuns are still visible as diminutive, circular pock marks. Unfortunately, these pock marks are not distinguishable as archaeological features when compared to the surrounding topography. However, most chultuns have the best visibility in the hillshade model with 46% accuracy. Depressions are also best visible in the hillshade model with 64% accuracy (figure 7). The depressions have shallow sides; so more surface area is exposed. As a result, the shading is more obvious and easy to single out. Mounds have the highest accuracy at 80% and are most visible in the bonemap model with 72% accuracy (figure 8). The mounds identified in this study do not incline gradually, but rather are characterized by steep banks that stand out in slope models, and thus are even more apparent in the bonemap when those slope values are stretched. Platforms and quarries (figure 9) are also most visible in the bonemap model with accuracies ranging from 61% to 68%. Due to more complex shading constraints, the bonemap model is best for displaying smaller features like platforms and quarries. Terraces are most visible in the slope layer with 65% accuracy (figure 10). Since terraces are usually sequences of adjacent lines in LiDAR models, it is typically easy to note the striae in all models. However, they are displayed much more visibly in the slope model because of the high contrast and dark colors representing the low values that surround them. Note that the percentages of rejected features and LiDAR unidentified features overall are very low, indicating that LiDAR is indeed a very effective medium for the remote sensing of archaeological landscapes. Also, it is important to realize that the percentages of LiDAR identified features are very high even though a lot of those features aren't validated after the groundtruthing process. On the basis of these findings, it is abundantly clear that LiDAR is extremely capable of revealing the ground surface, even through the thick canopy of the Maya Forest. The images below are ordered from lowest visibility to highest visibility. Depressions are clearly more detectable in the hillshade LiDAR rendering because hillshade takes the sun's relative position into account resulting in a smoother surface. Features that have higher altitudes or lower depths (such as depressions) are thus displayed more clearly because they are either brightly illuminated or they cast a discernable shadow. Features like mounds and quarries are often small and are more difficult to detect in LiDAR models. However, the bonemap displays these features more clearly than in the other two models. This is because the bonemap is derived from the slope map, which displays even the subtlest degrees of inclination using the digital elevation model as a proxy. Since the slope values in a bonemap are stretched and since the black to white color scheme is inverted, smaller features have a much higher visibility. Raw slope map values though are darker with the higher values represented by lighter color. Because of this, features with subtle elevation distinguishability (such as terraces)

are more visible. The bonemap is less effective in displaying terraces because the inverted color scheme results in light colored low values, making subtle features more difficult to detect.

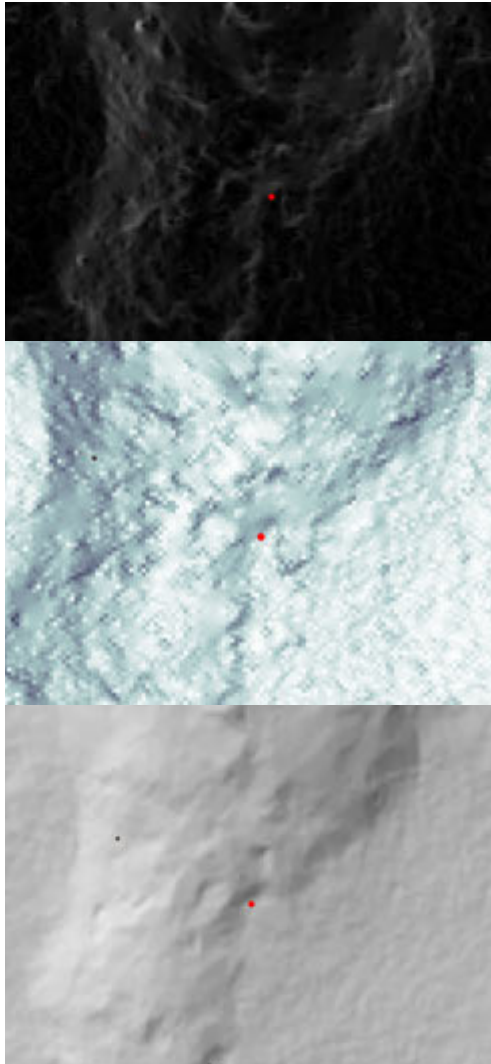


Figure 7: illustrates depressions in the three LiDAR models ranging from least visible (top image) to the most visible (bottom image). The red point is located in the approximate center of the feature.

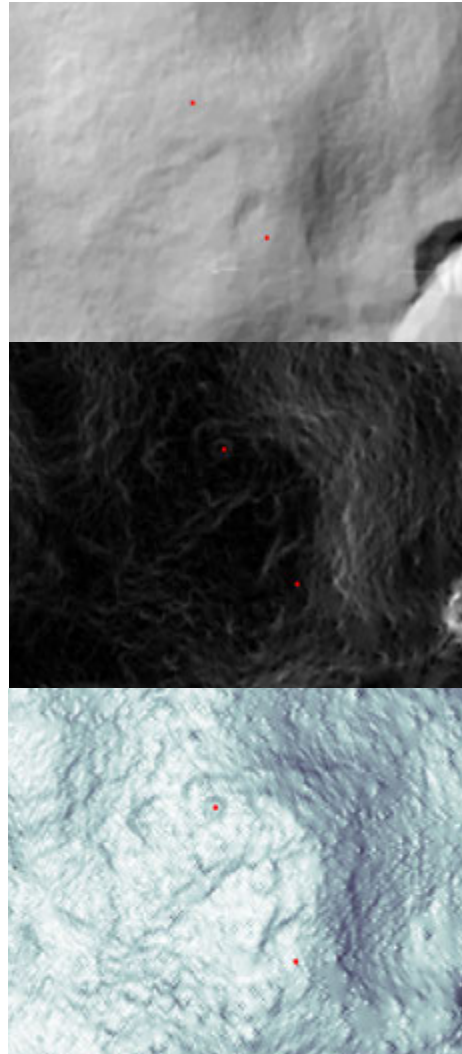


Figure 8: illustrates mounds in the three LiDAR models ranging from least visible (top image) to the most visible (bottom image). The red point is located in the approximate center of the feature.

Discussion

In the evaluation of Maya archaeological features and their visibility in LiDAR models, the results indicate that while certain models are more appropriate for displaying unique feature types, when LiDAR is used in archaeological feature detection, ALL maps (slope, hillshade, and bonemap) should be meticulously scanned for EACH feature. Features in the same typology

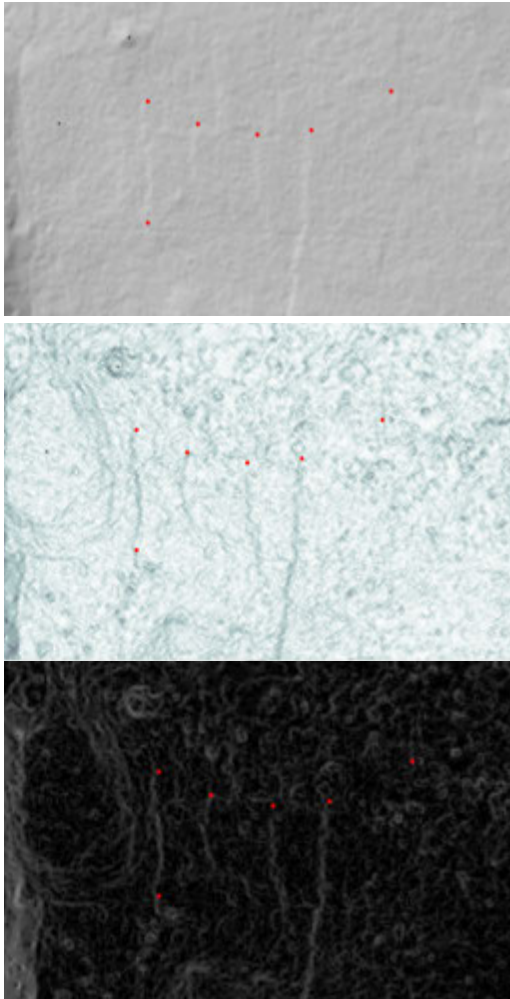


Figure 9 shows terraces in the three LiDAR models ranging from least visible (top image) to the most visible (bottom image). The red dots are located to one side or on both sides of the terraces.

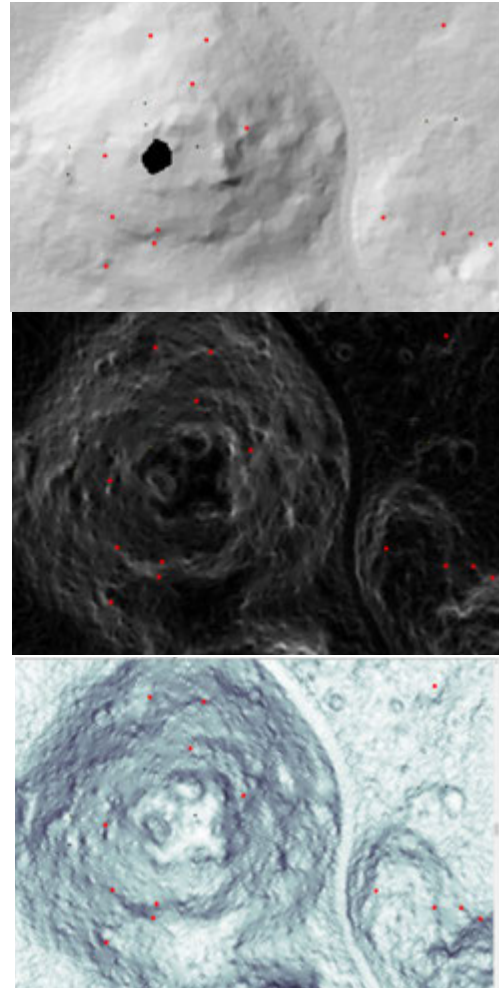


Figure 10 shows quarries in the three LiDAR models ranging from least visible (top image) to the most visible (bottom image). The quarries are difficult to see even in the bonemap because they are small and hard to recognize as distinct archaeological features. The red dots are located in the approximate center of the feature.

were not constructed in exactly the same way as other features. Furthermore, those features are not in the same spatial location. Features might be located in uplands or lowlands, on hills or on level terrain. Features might also be next to or on top of other features. Platforms for instance are almost always adjacent to mounds, though most mounds are not near platforms. Hence archaeological features won't always be visible or noticeable in the expected model. A multi-modal approach is necessary to maximize feature detection. An individual model, while effective to an extent, can produce error by obscuring critical features. It is also important to consider the statistics of feature visibility in the three models. Visibility percentages are neither extremely high nor extremely low, suggesting that neither of the three models should be used exclusively. Used in conjunction though, these LiDAR models are powerful and accurate tools for discovering and identifying features on the ground surface. Hillshaded DEM images are

capable of revealing numerous feature types including terraces (Chase et al. 2010). Bonemaps have the advantage of displaying most feature types compared to other processed LiDAR models, which is consistent with Pingel and Clarke’s findings (Pingel et al. 2015), but extend them by comparing them to different feature types. And the unstretched slope map is capable of revealing small or narrow, steep-sloped features. The fact that even the most diminutive of features such as chultuns can be detected through an incredibly dense canopy speaks to the effectiveness and usefulness of LiDAR in archaeological applications. However, it is also important to take into account that there is an expected model (figure 11). When visually scanning LiDAR renderings, if one comes across a questionable feature, one can assume typology based on that feature’s visibility. While these assumptions should not be used exclusively as a basis for feature identification, they certainly add weight and more information to field data findings. Also note that the bonemap LiDAR model is still the most effective model overall at displaying features beneath the canopy. The bonemap should thus be integrated into the spatial analysis of any archaeological site, especially sites with dense tree canopies. While relative feature size was not incorporated into this study, it has important implications for future research. By correlating the best LiDAR model for each feature type with a size range for those feature types, we should be able to create an algorithm that will automatically detect features and sort them into a typology with reasonable accuracy. This will allow for a much faster generation of LiDAR accepted points that can be sent into the field and subsequently groundtruthed. There are many different ways of processing raw LiDAR point clouds to display information differently. However, for Maya archaeological features, the hillshade, slope, and bonemap models are essential tools and they should be used by archaeologists and surveyors to their full extent.

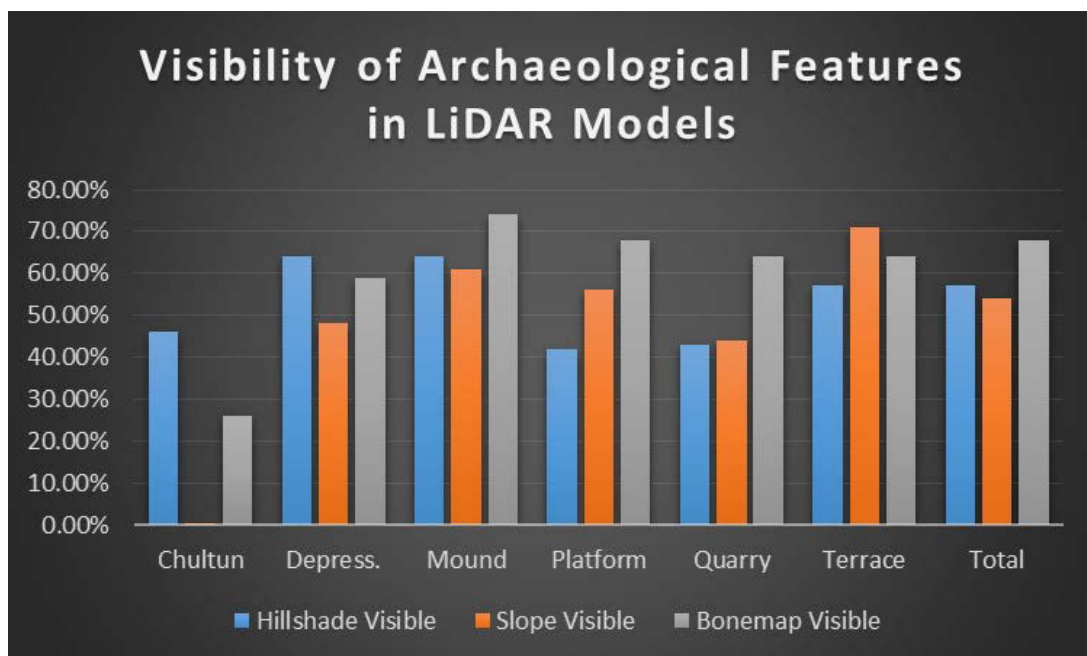


Figure 11: This is a representation of feature types and the percentages of their visibility in juxtaposition to one another to show an expected model of LiDAR raster accuracy in Maya archaeological sites.

References

- Chase, A.F., D.Z. Chase, J.F. Weishampel, J.B. Drake, R.L. Shrestha, K. Slatton, A. Clint, J. Jaime, W.E. Carter (2010) Airborne LiDAR, archaeology, and the ancient Maya landscape at Caracol, Belize
- Pingel, T.J., K. Clarke and A. Ford (2015) Bonemapping: a LiDAR processing and visualization technique in support of archaeology under the canopy, *Cartography and Geographic Information Science*, 42(1): 18-26, DOI:10.1080/15230406.2015.1059171
- Whittaker, J.C., K.A. Kamp, A. Ford, R. Guerra, P. Brands, J. Guerra, K. McLean, A. Woods, M. Badillo, J. Thornton and Z. Eiley (2009) Lithic industry in a Maya center: An axe workshop at El Pilar, Belize. *Latin American Antiquity* 20(1): 134-156. URL: <http://www.jstor.org/stable/40650080>
- Coluzzi, R., N. Masini, and R. Lasaponara (2011) Flights into the past: full-waveform airborne laser scanning data for archaeological investigation. *Journal of Archaeological Science* 38: 2061–2070.
- Doneus, M., C. Briese, M. Fera, M. Janner (2008) Archaeological prospection of forested areas using full-waveform airborne laser scanning. *Journal of Archaeological Science* 35: 882–893.
- Stular, B., Z. Kokalj, K. Ostir, L. Nuninger (2012) Visualization of lidar-derived relief models for detection of archaeological features. *Journal of Archaeological Science* 39:3354-3360.
- Weiss-Krejci, E. and T. Sabbas (2002) The Potential Role of Small Depressions as Water Storage Features in the Central Maya Lowlands. *Latin American Antiquity* 13(3): 343-357.
- Ford, A. and S. Fedick (1992) Prehistoric Maya Settlement Patterns in the Upper Belize River Area: Initial Results of the Belize River Archaeological Settlement Survey. *Journal of Field Archaeology* 19(1): 35-49.
- Healy, P.F., J.D.H. Lambert, J.T. Arnason and R.J. Hebda (1983) Caracol, Belize: Evidence of Ancient Maya Agricultural Terraces. *Journal of Field Archaeology* 10(4): 397-410.

Richard K. Ellsworth, Research Fellow, Department of Geography, The University of California Santa Barbara, Santa Barbara, CA 93106 and Undergraduate Student, Department of Geography, The University of Connecticut, Storrs, CT 06269